Journal of Power Sources 196 (2011) 5792–5796

Contents lists available at ScienceDirect

Journal of Power Sources

journal homepage: www.elsevier.com/locate/jpowsour

Short communication

Down-converting lanthanide doped TiO_2 photoelectrodes for efficiency enhancement of dye-sensitized solar cells

H. Hafez [a], M. Saif [b,*], M.S.A. Abdel-Mottaleb [c]

[a] Environmental Studies and Research Institute (ESRI), Minoufiya University, Sadat Branch, Sadat City, Egypt
[b] Department of Chemistry, Faculty of Education, Ain Shams University, Roxy, Cairo, Egypt
[c] Nano-Photochemistry and Solarchemistry Lab., Department of Chemistry, Faculty of Science, Ain Shams University, Abbassia, 11566 Cairo, Egypt

ARTICLE INFO

Article history:
Received 18 December 2010
Received in revised form 3 February 2011
Accepted 13 February 2011
Available online 21 February 2011

Keywords:
Dye-sensitized solar cells
Lanthanide ions
Down-conversion

ABSTRACT

Lanthanide (Ln^{3+}) doped TiO_2 down-conversion photoelectrodes ($Ln^{3+} = Eu^{3+}$ and Sm^{3+} ions) are used to enhance the photovoltaic efficiency of dye-sensitized solar cells (DSSC). We report on achieving fill factors of 0.67 and 0.69 and efficiencies of 5.81% and 5.16% for Sm^{3+} and Eu^{3+}, respectively. This is compared to the 4.23% efficiency for the undoped-titania photoelectrodes. This enhancement is probably due to the improved UV radiation harvesting via a down-conversion luminescence process by the lanthanide ions. The structure, optical and photoluminescence properties of the down-converting photoelectrode are characterized by X-ray diffraction (XRD), scanning electron microscope (SEM), energy dispersive X-ray (EDX) and room temperature photoluminescence excitation and emission spectrofluorimetric measurements.

1. Introduction

Recently, clean renewable energy utilization has been proposed as one of the main potential solutions for global warming [1]. Silicon-based solar cell technology is the most dominate technology in the current market of solar energy. Due to its relatively high cost and complicated fabrication methodology, developing a low-cost and highly efficient alternative technology has received a great deal of attention in the past decade [2]. In 1991, O'Reagan and Grätzel designed the first dye-sensitized solar cell (DSSC) [3]. Because of its low cost and simple fabrication methodology, improving DSSC efficiency has become of significant importance for many research groups worldwide. In DSSCs, TiO_2 films with mesoscopic texture are widely used as the photoanode onto which dye-sensitizers are adsorbed. Under illumination, excited dye-molecules inject electrons into the conduction band of the semiconductor. Injected electrons are then transported to the conducting glass substrate [4].

Generally, DSSCs have maximum absorption up to 800 nm of the total incident solar irradiation [5,6]. This represents a major issue for this technology, since 50% of solar irradiation is in the ultraviolet and infrared regions, and thus is not utilized. This limits the solar energy conversion efficiency for DSSCs. Therefore, attempting to extend the spectral response range of a DSSC to the UV region represents an extremely important approach to increasing the DSSC efficiency.

Preliminary encouraging results in our laboratory encouraged us to carry out further investigations to explore the possibility of modifying the spectral response of DSSCs by the use of down-conversion lanthanide-doped TiO_2 photoelectrodes.

Lanthanide-derived compounds have been widely used as highly efficient light conversion molecular devices (LCMD), magnets and catalysts based on the electronic, optical, and chemical characteristics arising from their 4f electrons [6,7]. Among the many lanthanide ions, europium (Eu^{3+}) and samarium (Sm^{3+}) ions have been recognized as the most efficient down-converting materials that convert the ultraviolet light to red and orange-red emissions, respectively [7,8]. Intermolecular energy transfer process from the host material, which absorbs the UV energy to the central lanthanide cation results in the observed visible light emission [8]. Moreover, doping of titania electrode with lanthanide ions provide complexation centers on the TiO_2 surface, thus enhancing its dye adsorption ability [9].

In the current work, we have investigated the role of new down-converter Eu^{3+} or Sm^{3+} -doped TiO_2 photoelectrode on the photovoltaic efficiency enhancement of dye-sensitized solar cells.

2. Experimental

2.1. Materials

Chemical agents including tetraisopropyl titanate $Ti[OCH(CH_3)_2]_4$, samarium nitrate $Sm(NO_3)_3$ and europium

* Corresponding author. Tel.: +20 109542296; fax: +20 22581243.
E-mail address: mona_saif1@yahoo.com (M. Saif).

0378-7753/$ – see front matter © 2011 Elsevier B.V. All rights reserved.
doi:10.1016/j.jpowsour.2011.02.031

nitrate $Eu(NO_3)_3$, iodine I_2, lithium iodide LiI, 4-tert-butylpyridine (TBP) and tetrapropylammonium iodide $N(n\text{-}C_3H_7)_4I$ were purchased from (Sigma Aldrich, NY, USA) and used as received. The p-octyl polyethylene glycol phenyl ether (OP) emulsification agent (Triton X-100), polyethylene glycol 20,000 and cyanoacrylate adhesive were purchased from the above company and used without further treatment. Other organic solvents such as ethanol and acetonitrile were of analytical grade and were used without further purification. Conducting glass plates with a fluorine-doped indium tin oxide (FTO) glass overlayer, sheet resistance (25 $\Omega\,cm^{-2}$) was purchased from Hartford Glass Co. USA. The sensitizing dye N-719 [$RuL_2(NCS)_2$, L = 4,4-dicarboxylate-2,2-bipyridine] was purchased from Solaronix, SA.

2.2. Preparation of Ln^{3+}-doped-TiO_2 nanoparticles

Nanoporous Sm^{3+} and Eu^{3+}-doped and undoped TiO_2 films were prepared by the sol–gel method described by Flores and Wang [10,11]. In a typical method, titanium isopropoxide (TIIP) (8 ml) was rapidly added to distilled water (100 ml) and a white precipitate was formed immediately. The precipitate was filtered using a glass frit and washed three times with 100 ml of distilled water. The filter cake was added to nitric acid aqueous solution (0.1 M, 160 ml) under vigorous stirring at 80 °C until the slurry became a translucent blue-white liquid. Then 5 wt% of lanthanide salts was added to the above solution under stirring for one more hour. The resultant colloidal suspension was autoclaved at 200 °C for 12 h to form milky white slurry. The resultant slurry was concentrated to 1/4 of its volume, then PEG-20000 (10 wt% slurry) and a few drops of emulsification regent of Triton X 100 were added to form a TiO_2 colloid.

2.3. DSSC fabrication

Ln^{3+} doped TiO_2 nanoparticle photoelectrodes of approximately 9 μm thickness and 0.2 cm^2 active area, were coated using doctor-blading technique [12–15]. After air drying, the electrode was sintered at 450 °C for 30 min, then cooled down to 80 °C. To absorb the dye, the calcined titania electrode was immersed in ethanol solution of 2.5×10^{-4} M dye solution for 24 h. After the substrate was adequately washed with anhydrous alcohol and dried in moisture free air, the dye-sensitized TiO_2 electrode was obtained. A DSSC was assembled by filling an electrolyte solution (0.6 M tetrapropylammonium iodide, 0.1 M iodine, 0.1 M lithium iodide, 0.5 M 4-tertbutylpyridine (TBP) in acetonitrile) between the dye-sensitized TiO_2 electrode and a platinized conducting glass electrode. The two electrodes were clipped together, and a cyanoacrylate adhesive was used as sealant to prevent the electrolyte solution from leaking.

2.4. Characterization

The crystal structure of the doped and un-doped titania electrodes was identified by X-ray diffraction (XRD) on D/max γA X-ray diffractometer (X· Pert Pro, Japan) with Cu Kα radiation (K_α = 0.15418 nm) at 45 kV and 40 mA. The room-temperature photoluminescence (PL) excitation and emission spectra of the samples were recorded with SHIMADZU RF-5301, PC spectrofluorophotometer using a Xe lamp as the excitation source. The morphology of the TiO_2:Eu^{3+} and TiO_2:Sm^{3+} photoactive electrodes were observed with a Field-Emission Environmental scanning electron microscope FESEM (Philips XL30, 109 Japan) connected with EDX detector unit.

The photovoltaic testing of DSSCs was carried out by measuring the *J–V* character curves using a Keithley 2635 device, under simulated AM 1.5 solar illumination at 100 mW cm^{-2} from a xenon arc lamp (CHF-XM500, Trusttech Co., Ltd., China) in ambient atmosphere. The fill factor (FF) and overall light-to-electrical energy conversion efficiency (η) of DSSC were calculated according to the following equations [16]:

$$FF = \frac{V_{max} \times J_{max}}{V_{OC} \times J_{SC}} \quad (1)$$

$$\eta(\%) = \frac{V_{max} \times J_{max}}{P_{in}} \times 100 = \frac{V_{OC} \times J_{SC} \times FF}{P_{in}} \times 100 \quad (2)$$

where J_{SC} is the short-circuit current density (mA cm^{-2}), V_{OC} is the open-circuit voltage (V), P_{in} is the incident light power, and J_{max} (mA cm^{-2}) and V_{max} (V) are the current density and voltage at the point of maximum power output on the *J–V* curves, respectively.

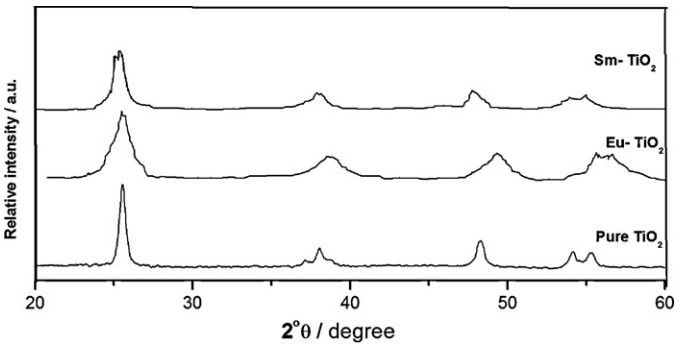

Fig. 1. XRD pattern of pure TiO_2 and 5% Ln^{3+}/TiO_2 thin films calcined at 450 °C for 30 min in air.

3. Results and discussion

3.1. Structure and morphology characterizations

Fig. 1 shows the XRD pattern of pure TiO_2, Eu^{3+}-doped TiO_2 and Sm^{3+}-doped TiO_2 thin films. The XRD peaks at 2θ = 25.5°, 38.7°, 48.1° and 54.2° in the spectra of un-doped and doped thin films are easily identified as a relatively high crystallinity anatase form (JCPDS 21-1272). Additionally, it has been found that all doped thin films showed broader diffraction peaks than the undoped TiO_2 due to smaller grain sizes (Fig. 1) [9,17–19].

In Fig. 2a SEM analysis shows that pure TiO_2 exhibits a uniform surface morphology without any cracks. Similar images were also obtained for both Sm^{3+} and Eu^{3+}-doped TiO_2. The thickness of the film, which is an important parameter for the evaluation of DSSC efficiency constructed with such film, was measured to be approximately 9 ± 1 μm. To investigate the elemental composition of doped and undoped TiO_2 thin films, energy dispersive X-ray (EDX) analysis was carried out. As shown in Fig. 2b the EDX spectrum of the pure TiO_2 thin film shows strong K_α and K_β diffraction peaks from Ti element appearing at 4.51 and 4.92 keV, and a slender peak of the element O appears at 0.533 keV [20]. For Eu^{3+} doped TiO_2 and Sm^{3+}doped TiO_2 thin films, in addition to the above diffraction peaks, new diffraction peaks for Eu and Sm also appear in their EDX spectra (Fig. 2c and d), which proves the presence of Eu^{3+} or Sm^{3+} in TiO_2 nanoparticle thin films [6].

3.2. Photoluminescence characteristics (PL)

The room temperature PL excitation and emission spectra of Eu^{3+}-doped TiO_2 and Sm^{3+}-doped TiO_2 thin films are measured to illustrate the down-conversion process and are depicted in Fig. 3(a–d). The PL excitation spectrum of Eu^{3+}-doped TiO_2 thin film shows typical direct excitation peaks due to the $^7F_0$–^5L_J transition of Eu^{3+} at around 396 nm and a peak from the $^7F_0$–$^5D_2$ transition of

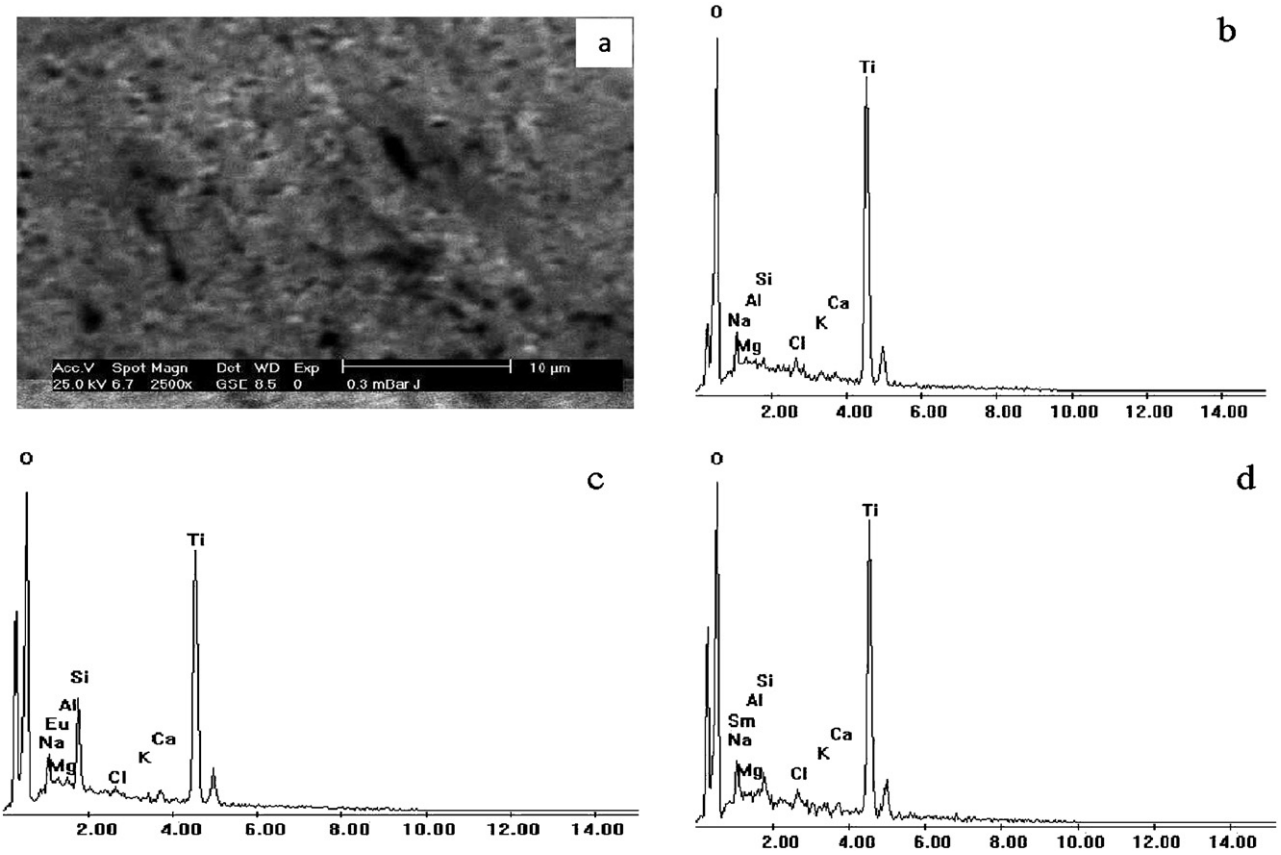

Fig. 2. (a) Top view SEM image of pure TiO_2 thin film, (b) EDX spectrum of pure TiO_2, (c) EDX spectrum of 5% Eu^{3+}doped-TiO_2 and (d) EDX spectrum 5% Sm^{3+}/TiO_2 thin films.

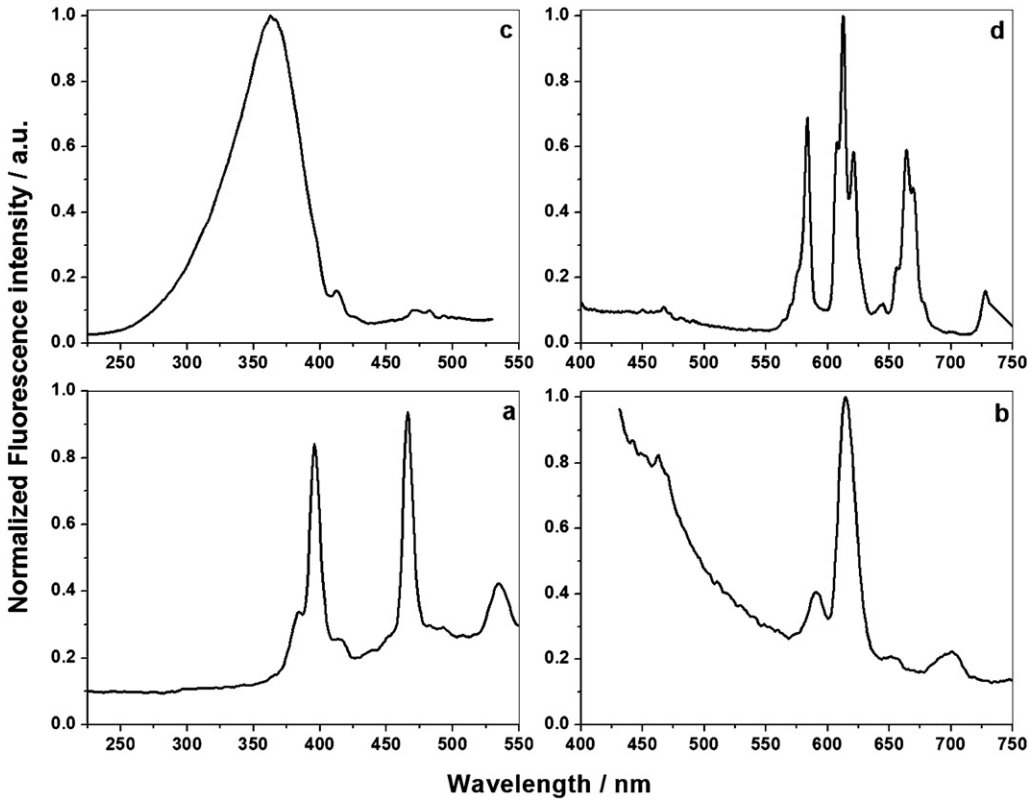

Fig. 3. Excitation and emission spectra of 5% Eu^{3+}doped-TiO_2 (λ_{em} = 614 nm and λ_{ex} = 395 nm) (a and b) and 5% Sm^{3+}/TiO_2 thin films (λ_{em} = 613 nm and λ_{ex} = 370 nm) (c and d).

Eu^{3+} at around 467 nm. These peaks are attributed to intra 4f transitions (Fig. 3a) [21]. Additionally, in this PL excitation spectrum, the little shoulder peak at 385 nm (3.22 eV) corresponds to the energy gap of TiO_2. These results clearly indicate that the Eu^{3+} ions can be excited with UV light either indirectly through the TiO_2 host lattice or directly through absorption by Eu^{3+} ions themselves [22].

Fig. 3b shows the characteristic visible PL emission bands of Eu^{3+}-doped TiO_2 under UV excitation located at 575, 591, 615, 652, and 700 nm. These bands corresponding to the $^5D_0$–$^7F_0$, $^5D_0$–$^7F_1$, $^5D_0$–$^7F_2$, $^5D_0$–$^7F_3$ and $^5D_0$–$^7F_4$ transitions, respectively. Furthermore, a broad emission band observed at 450 nm in the Eu^{3+}-doped TiO_2 spectrum could be attributed to TiO_2 in the composites [23]. The $^5D_0$–$^7F_0$ transition is strictly forbidden by symmetry. Since the forbidden $^5D_0$–$^7F_0$ transition is observed; the spectrum indicates that Eu^{3+} occupies sites with low symmetry and no inversion center, which is consistent with the crystal structures. The $^5D_0$–$^7F_1$ and $^5D_0$–$^7F_2$ transitions, which correspond to magnetic and electric dipole transitions, respectively, are clearly observed in the photoluminescence spectrum of Eu^{3+}/TiO_2.

It is well known that the $I(^5D_0$–$^7F_2)/I(^5D_0$–$^7F_1)$ asymmetry ratio (R) is widely used as a measure of the coordination state and site symmetry of the rare earth. The R value is equal to 2.37, which also indicates the low site symmetry of the Eu^{3+} ion, and the intense $^5D_0$–$^7F_2$ transition points to a highly polarizable chemical environment around the Eu^{3+} ion that is responsible for the brilliant red emission of the compound [24]. However, the present value of R does not agree with the relatively high symmetry of the Ti^{4+} ions in the anatase structure (D_{2d}), as this symmetry is not compatible with a hypersensitive behavior of the $^5D_0$–$^7F_2$ transition. This indicates that the Eu^{3+} ion does not substitute for Ti^{4+} without a significant site distortion [25]. The presence of such disorder is ascribed to the significant difference in the ionic radii in six-fold coordination for Ti^{4+} (0.64 Å) and Eu^{3+} (1.036 Å) [25].

The PL excitation spectrum of Sm^{3+}-doped TiO_2 thin film exhibits an intense broad band in the ultraviolet region centered at 363 nm, which is assigned to the band gab of anatase host absorption, confirming the effective energy transfer from TiO_2 host to Sm^{3+} ions. Weak bands at 412 and 470 nm are due to the direct excitation of Sm^{3+} (Fig. 3c) [26]. The emission spectrum shows the characteristic orange-red luminescence of the trivalent samarium ion upon UV excitation. The bands at 583, 613 and 664 nm are assigned to the electronic transition of $^4G_{5/2}$–$^6H_{5/2}$, $^4G_{5/2}$–$^6H_{7/2}$ and $^4G_{5/2}$–$^6H_{9/2}$ of Sm^{3+}, respectively (Fig. 3d) [27]. Moreover, the PL spectrum of Sm^{3+}-doped TiO_2 contains a weak broad emission band around 400–500 nm originating from defect of host, the intensity of the emission from Sm^{3+} is clearly stronger than that from the host emission. This also confirms that the efficient non-radiative energy transfer from surrounding Ti–O octahedron to Sm^{3+} ions is indeed effective in the Sm^{3+}-doped TiO_2 [28]. This fine structure can be explained by taking into account that the ^6H_J levels are split into 2J+1 sublevels in the crystal field. Although the radii of Ln^{3+} ions seem to be too large to allow them to replace Ti^{4+} in an anatase crystal (1.04 Å versus 0.64 Å), the well resolved ^6H_J levels clearly demonstrate that Sm^{3+} ions are fitted into the regular environment, contrary to the case in amorphous matrices. It is reasonable to conclude that the Sm^{3+} ion distorts the TiO_6 octahedron substituting the Ti^{4+} ion in shifted position [29]. Based on the model given by Frindell and Bartl [30], a modified model for the energy transfer in this doping system is proposed in Fig. 4. In Fig. 4, (1) the generation process of excitons upon UV excitation, (2) the non-radiative energy transfer process from an exciton to defect states, (3) the non-radiative energy transfer process from defect states to Ln^{3+}, and (4) the emission process of Ln^{3+} [27–29]. So the PL measurements confirm that the lanthanide doped titania thin film can be used as effective down-conversion materials for harvesting UV light from solar radiation into visible range.

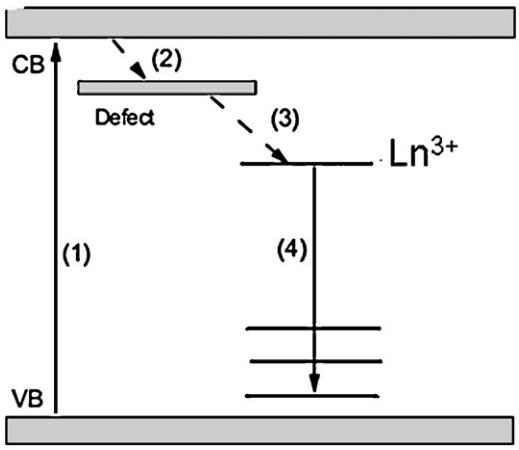

Fig. 4. Schematic of photoluminescence processes in Ln^{3+}/TiO_2 thin film.

3.3. Photovoltaic characteristics and performance

The photocurrent–voltage properties of DSSCs with different doped and undoped titania electrodes were measured and shown in Fig. 5. The open-circuit voltage (V_{oc}), short circuit current density (J_{sc}), fill factor (FF) and overall light-to-electrical energy conversion efficiency (η) of these DSSCs are summarized in Table 1. The DSSCs with Sm^{3+} and Eu^{3+}-doped TiO_2 thin film electrodes shows a conversion efficiency of 5.81%, and 5.16%, respectively, which is higher than that of the pure TiO_2 film electrode (η = 4.23%). The enhancement in the overall efficiency that has been achieved by doping of the titania electrode by the rare earth; Sm (34%) and Eu ions (22%), is mainly due to the down-conversion luminescence characteristics of Sm^{3+} and Eu^{3+} ions, which has been confirmed from the above PL measurements of the lanthanide doped titania film. However, the doping with the Sm ions leads to higher improvement in the overall efficiency of the DSSC than Eu ions. This can be attributed to the smaller lifetime values of Sm than that of Eu published elsewhere [31–34], which reflecting enhanced light energy transfer in case of Sm^{3+} to its surroundings.

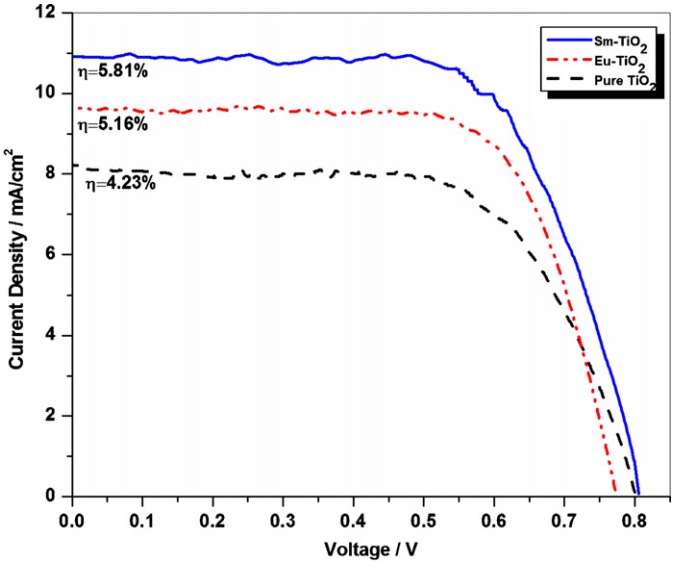

Fig. 5. *J–V* curves for DSSCs with different electrodes.

Table 1
The parameters of the dye-sensitized solar cells with different electrodes.

Electrode	V_{oc} (V)	J_{sc} (mA cm^{-2})	V_{max} (V)	J_{max} (mA cm^{-2})	FF	η%
Undoped TiO_2	0.80	8.32	0.57	7.43	0.64	4.23
Eu^{3+}-doped TiO_2	0.77	9.61	0.57	9.05	0.69	5.16
Sm^{3+}-doped TiO_2	0.81	10.9	0.57	10.4	0.67	5.81

4. Conclusions

Thin film down-conversion Sm^{3+}-doped TiO_2 and Eu^{3+}-doped TiO_2 electrodes were prepared, characterized and used to fabricate a more efficient dye-sensitized solar cells compared with DSSC based on pure TiO_2 photoactive electrode.

References

[1] A. Kumar, T.C. Kandpa, Energy 32 (2007) 861–870.
[2] L.L. Tobin, T. O'Reilly, D. Zerulla, J.T. Sheridan, Optik- Int. J. Light Electron Opt., in press.
[3] B. O'Reagan, M. Grätzel, Nature 353 (1991) 737–739.
[4] Q. Yao, J. Liu, Q. Peng, X. Wang, Y. Li, Chem. Asian J. 1 (2006) 737–741.
[5] T. Ono, T. Yamaguchi, H. Arakawa, Sol. Energy Mater. Sol. Cells 93 (2009) 831–835.
[6] H. Hafez, J. Wu, Z. Lan, Q. Li, G. Xie, J. Lin, M. Huang, Y. Huang, M.S.A. Abdel-Mottaleb, Nanotechnology 21 (2010) 415201–415206.
[7] M. Saif, J. Photochem. Photobiol. A: Chem. 205 (2009) 145–150.
[8] H.-Y. Li, J. Wu, W. Huanga, Y.-H. Zhou, H.-R. Li, Y.-X. Zheng, J.-L. Zuo, J. Photochem. Photobiol. A: Chem. 208 (2009) 110–116.
[9] M. Saif, M.S.A. Abdel-Mottaleb, Chim. Acta 360 (2007) 2863–2874.
[10] W. Wang, W. Widiyastuti, T. Ogi, W. Lenggoro, K. Okuyama, Chem. Mater. 19 (2007) 1723–1730.
[11] I. Flores, J. Freitas, C. Longo, M. Paoli, H. Winnischofer, A. Nogueira, J. Photochem. Photobiol. A: Chem. 189 (2007) 153–160.
[12] J. Wu, S. Hao, Z. Lan, J. Lin, M. Huang, Y. Huang, P. Li, S. Yin, T. Sato, J. Am. Chem. Soc. 130 (2008) 11568–11569.
[13] J. Wu, S. Hao, J. Lin, M. Huang, Y. Huang, Z. Lan, P. Li, Cryst. Growth Des. 8 (2008) 247–252.
[14] Z. Lan, J. Wu, J. Lin, M. Huang, S. Yin, T. Sato, Electrochim. Acta 52 (2007) 6673–6678.
[15] H. Hafez, Z. Lan, Q. Li, J. Wu, Nanotechnol. Sci. Appl. 3 (2010) 45–51.
[16] M. Gratzel, Prog. Photovoltaics 8 (2000) 171–185.
[17] Hoda S. Hafez, M. Saif, James T. McLeskey Jr., M.S.A. Abdel Mottaleb, I.S. Yahia, T. Story, W. Knoff, Int. J. Photoenergy 2009 (2009) 1–8.
[18] S. Pavasupree, S. Ngamsinlapasathian, M. Nakajima, Y. Suzuki, S. Yoshikawa, Photochem. Photobiol. A: Chem. 184 (2006) 163–169.
[19] J. Li, X. Yang, X. Yu, L. Xu, W. Kang, W. Yan, H. Gao, Z. Liu, Y. Guo, Appl. Surf. Sci. 255 (2009) 3731–3738.
[20] Z. Zhang, Y. Yuan, L. Liang, Y. Cheng, H. Xu, G. Shi, L. Jin, Thin Solid Films 516 (2008) 8663–8667.
[21] D.H. Park, S.H. Cho, J.S. Kim, K. Sohn, J. Alloys Compd. 449 (2008) 196–201.
[22] J. Li, X. Wang, K. Watanabe, T. Ishigaki, J. Phys. Chem. B 110 (2006) 1121–1127.
[23] Z. Liu, J. Zhang, B. Han, J. Du, T. Mu, Y. Wang, Z. Sun, Micropor. Mesopor. Mater. 81 (2005) 169–174.
[24] N.V. Gaponenko, I.S. Molchan, G.E. Thompson, P. Skeldon, A. Pakes, R. Kudrawiec, L. Bryja, J. Misiewicz, Sens. Actuators A 99 (2002) 71–73.
[25] D. Falcomer, M. Daldosso, C. Cannas, A. Musinu, B. Lasio, S. Enzo, A. Speghini, M. Bettinelli, J. Solid State Chem. 179 (2006) 2452–2457.
[26] V. Kiisk, M. Šavel, V. Reedo, A. Lukner, I. Sildos, Phys. Procedia 2 (2009) 527–538.
[27] M. Ikeda, J. Li, N. Kobayashi, Y. Moriyoshi, H. Hamanaka, T. Ishigaki, Thin Solid Films 516 (2008) 6640–6644.
[28] J. Yin, X. Zhao, Mater. Chem. Phys. 114 (2009) 561–568.
[29] C. Gao, H. Song, L. Hu, G. Pan, R. Qin, F. Wang, Q. Dai, L. Fan, L. Liu, H. Liu, J. Lumin. 128 (2008) 559–564.
[30] K.L. Frindell, M.H. Bartl, J. Solid State Chem. 172 (2003) 81–87.
[31] H. Wang, J. Yang, C.M. Zhang, J. Lin, J. Solid State Chem. 182 (2009) 2716–2724.
[32] J. Wu, H. Li, Q. Xu, Y. Zhu, Y. Tao, H. Li, Y. Zheng, J. Zuo, X. You, Inorg. Chim. Acta 363 (2010) 2394–2400.
[33] H. Li, J. Wu, W. Huang, Y. Zhou, H. Li, Y. Zheng, J. Zuo, J. Photochem. Photobiol. A: Chem. 208 (2009) 110–116.
[34] P.A. Tanner, C. Duan, V.N. Makhov, M. Kirm, N.M. Khaidukov, Optic. Mater. 31 (2009) 1729–1734.